A New Performance Index for Underactuated Cable-Driven Parallel Robots

Edoardo Idà[1 [0000−0003−0437−4651]] and Marco Carricato[1 [0000−0002−1528−4304]]

University of Bologna, Department of Industrial Engineering, Bologna, Italy
{edoardo.ida2,marco.carricato}unibo.it, http://www.irmalab.org/

Abstract. Cable-driven parallel robots (*CDPRs*) equipped with less cables than the end-effector (*EE*) degrees of freedom (*DoFs*) are underactued and underconstrained by design. These characteristics imply that only a subset of the *EE DoFs* can be assigned for planning purposes, and that the *EE* can freely move when actuators are locked. The performance of this class of manipulators has yet to be fully analyzed, since common performance indices for fully or redundantly actuated robots may not directly apply. In this paper, a novel index is proposed, which is tailored for *suspended* underactuated *CDPRs*. This index analyses cable-tension sensitivity to cable-length variation, and aims at determining if a static equilibrium configuration is attainable under bounded cable-length control errors. When 4- or 5-cable *UACDPRs* have to perform positioning tasks, the optimization of such an index may be used to determine the safest *EE* orientation with respect to actuation errors.

Keywords: Underactuated cable-driven parallel robots, Underconstrained cable-driven parallel robot, performance index, trajectory optimization.

1 Introduction

Underactuated Cable-driven parallel robots (underactuated *CDPRs*, or *UACDPRs* in short) control the end-effector (*EE*) pose by means of n extendable cables, whose number is smaller than the *EE* degrees of freedom (*DoFs*). *UACDPRs* are intrinsically underconstrained [1], since their *EE* is subject to less constaint actions than the number of its *DoFs*. As a consequence, only a subset of the *EE* coordinates can be directly controlled, and the *EE* preserves some freedoms once the actuators are locked. Given the reduced mechanical complexity and increased workspace accessibility of *UACDPRs*, a growing number of studies are being conducted on these systems in the field of trajectory planning [2–5], geometrico-static modeling [6], control [7], calibration [8], and workspace analysis [9]. On the other hand, *UACDPRs* performance evaluation is still an open problem.

Robot performance indices have been vastly investigated [10], and a few specific studies exist on their application to suspended, completely actuated *CDPRs*: the *global conditioning index* was used in [11] to evaluate the kinematic dexterity performance of a generic 6-cable *CDPR*; *rotation* and *displacement sensitivity to actuator displacement errors* were investigated in [12] for translational *CDPRs* and in [13] for

rotational *CDPRs*. As far as redundantly constrained *CDPRs* are concerned, the ratio between maximum and minimum cable tensions was introduced in [14] (called *tension factor* in [15]); the *maximum acceptable horizontal distance between the platform reference point and the center of mass of the set composed of the platform and a payload* was introduced in [16] to determine whether a handling task was feasible; and the maximum wrench that can be applied in a given direction, the *wrench exertion capability*, was explored in [17].

In this paper, a novel index for the evaluation of the geometrico-static performance of *UACDPRs* is introduced. This index, called *maximum tension variation under a cable displacement error*, aims at analysing the influence of actuator errors on *UACDPRs* static cable tensions. This analysis allows one to determine whether an equilibrium configuration may be safely attained under bounded cable-length control errors, with cables remaining likely taut. In addition, if 4- or 5-cable *UACDPRs* have to perform positioning tasks and the additional cables are used only to widen their static reachable workspace, the optimization of such an index could be used to determine the safest *EE* orientation with respect to actuation errors.

This paper is structured as follows. Section 2 recalls the geometrico-static model of *UACDPRs* with massless straight cables. Section 3 introduces the *maximum tension variation under a cable displacement error* index, based on the differential analysis of the geometrico-static model. An application is proposed in Sec. 4, where the orientation of a 4-cable *UACDPR* for a given reference position is determined as the one that minimizes the new index. In the end, conclusions and future works are discussed in Sec. 5.

2 Geometrico-Static Model

A *UACDPR* consists of a mobile platform coupled to the base by $n < 6$ cables, which can be coiled and uncoiled by motorized winches. In the following, $Oxyz$ is an inertial frame, whereas $Gx'y'z'$ is a mobile frame attached to the moving platform center of mass. The *EE* pose is described by the position vector $\mathbf{p}$ of G, and the rotation matrix $\mathbf{R}$ (Fig. 1). In this paper, $\mathbf{R}$ is parametrized by a minimal set of angles $\boldsymbol{\epsilon} = [\phi, \theta, \chi]^T$. The platform generalized coordinates are thus $\boldsymbol{\zeta} = \left[\mathbf{p}^T \, \boldsymbol{\epsilon}^T\right]^T$.

2.1 Geometric model

For the sake of simplicity, we assume that the i-th cable is massless and rigid, and is guided into the workspace through an eyelet at point B_i, described in the inertial frame by vector $\mathbf{b}_i$, and attached to the platform in point A_i, described in the moving frame by (the constant) ${}^P\mathbf{a}'_i$, and in the inertial frame by $\mathbf{a}_i = \mathbf{p} + \mathbf{a}'_i = \mathbf{p} + \mathbf{R}\,{}^P\mathbf{a}'_i$, where $\mathbf{a}'_i = \mathbf{R}\,{}^P\mathbf{a}'_i$. The cable vector connecting points A_i and B_i is $\boldsymbol{\rho} = \mathbf{a}_i - \mathbf{b}_i$ and, if l_i is the length of the i-th cable and $(\cdot)$ indicates the scalar product between vectors, the geometric constraint imposed by the cable on the platform is:

$$\boldsymbol{\rho} \cdot \boldsymbol{\rho} - l_i^2 = 0 \tag{1}$$

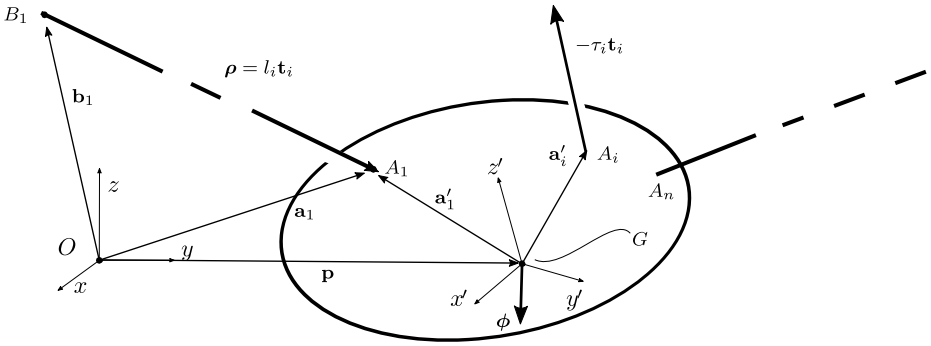

Fig. 1: *Geometrico-static model of the* UACDPR

2.2 Kinematic model

If $\boldsymbol{\omega}$ is the *EE* angular velocity, $\mathbf{v} = [\dot{\mathbf{p}}^T \boldsymbol{\omega}^T]^T$ the *EE* twist, $\mathbf{t}_i = \boldsymbol{\rho}_i / l_i$ the cable direction, and $(\times)$ indicates the vector product between vectors, differentiating Eq. (1) with respect to time yields:

$$\boldsymbol{\xi}_i \cdot \mathbf{v} - \dot{l}_i = 0, \qquad \boldsymbol{\xi}_i = \begin{bmatrix} \mathbf{t}_i \\ \mathbf{a}'_i \times \mathbf{t}_i \end{bmatrix}, \qquad i = 1, \ldots, n \tag{2}$$

The n relations in Eq. (2) can be grouped as::

$$\boldsymbol{\Xi}\mathbf{v} - \dot{\mathbf{l}} = \mathbf{0}_{n\times 1}, \qquad \dot{\mathbf{l}} = \begin{bmatrix} \dot{l}_1 & \cdots & \dot{l}_i & \cdots & \dot{l}_n \end{bmatrix}^T, \qquad \boldsymbol{\Xi} = \begin{bmatrix} \boldsymbol{\xi}_1 & \cdots & \boldsymbol{\xi}_i & \cdots & \boldsymbol{\xi}_n \end{bmatrix}^T \in \mathbb{R}^{n\times 6} \tag{3}$$

The *EE* twist $\mathbf{v}$ is related to the pose time derivative $\dot{\boldsymbol{\zeta}}$ through a matrix $\mathbf{D}$, whose formulation depends on the specific orientation parametrization employed and whose elements depend on the *EE* pose [4]:

$$\mathbf{v} = \mathbf{D}(\boldsymbol{\zeta})\dot{\boldsymbol{\zeta}} = \mathbf{D}\dot{\boldsymbol{\zeta}} \tag{4}$$

If Eq. (4) is substituted in Eq. (3), one gets:

$$\boldsymbol{\Xi}\mathbf{D}\dot{\boldsymbol{\zeta}} - \dot{\mathbf{l}} = \mathbf{J}\dot{\boldsymbol{\zeta}} - \dot{\mathbf{l}} = \mathbf{0}_{n\times 1}, \qquad \mathbf{J} = \boldsymbol{\Xi}\mathbf{D} \in \mathbb{R}^{n\times 6} \tag{5}$$

Matrices $\boldsymbol{\Xi}$ and $\mathbf{J}$ are the kinematic and analytical Jacobian matrices of the system and, since the robot is underactuated, they are rectangular; in case the manipulator is not in a singular configuration (whether a geometric or a representation one), $\text{rank}(\boldsymbol{\Xi}) = \text{rank}(\mathbf{J}) = n < 6$, which is strictly less than the number of *EE DoFs*. Thus, only n coordinates of the *EE* pose can be controlled by varying the *UACDPR* cable lengths, while the remaining $\lambda = 6 - n$ are to be determined according to the mechanical equilibrium of the platform. In addition, even if the actuators are locked and cable lengths are kept constant, λ freedoms remains. The *n controlled coordinates* are denoted as $\boldsymbol{\zeta}_c \in \mathbb{R}^n$, whereas the non-controllable coordinates will be referred to as *free coordinates* and denoted as $\boldsymbol{\zeta}_f \in \mathbb{R}^\lambda$. For simplicity sake, we will assume that the controlled coordinates are the first in the array $\boldsymbol{\zeta}$, that is, $\boldsymbol{\zeta} = [\boldsymbol{\zeta}_c^T \; \boldsymbol{\zeta}_f^T]^T$.

This coordinate partition is particularly useful in *trajectory planning* of *UACDPRs*, but it attains additional kinematic meaning. In fact, the *EE* twist $\mathbf{v}$ can be decomposed into two contributions, namely a *free twist*[1] $\mathbf{v}_f$ and a *controlled twist* $\mathbf{v}_c$, so that:

$$\mathbf{v} = \mathbf{v}_f + \mathbf{v}_c \tag{6}$$

The *free twist* is defined as the *EE* twist when the platform is in free motion, and it can be derived as the solution of Eq. (3) when $\dot{\mathbf{i}} = \mathbf{0}_{n\times 1}$, namely:

$$\boldsymbol{\Xi}\mathbf{v}_f = \mathbf{0}_{n\times 1} \tag{7}$$

The solution to Eq. (7) is readily obtained by considering the right nullspace $\boldsymbol{\Xi}^{\perp}$ of matrix $\boldsymbol{\Xi}$. By definition, the right nullspace of a $(n\times 6)$ matrix is a $(6\times\lambda)$ matrix such that $\boldsymbol{\Xi}\boldsymbol{\Xi}^{\perp} = \mathbf{0}_{n\times\lambda}$, thus its columns define a basis for the free twist $\mathbf{v}_f$:

$$\mathbf{v}_f = \boldsymbol{\Xi}^{\perp}\mathbf{c} \qquad \text{for some } \mathbf{c}\in\mathbb{R}^{\lambda} \tag{8}$$

If $\mathbf{J}^{\perp}$ is the right nullspace of matrix $\mathbf{J}$, we also have:

$$\boldsymbol{\Xi}\mathbf{v}_f = \boldsymbol{\Xi}\underbrace{\mathbf{D}\dot{\boldsymbol{\zeta}}}_{\mathbf{v}_f} = \underbrace{\boldsymbol{\Xi}\mathbf{D}}_{\mathbf{J}}\dot{\boldsymbol{\zeta}} = \mathbf{0}_{n\times 1} \qquad \Longrightarrow \qquad \dot{\boldsymbol{\zeta}} = \mathbf{J}^{\perp}\mathbf{c}' \quad \text{for some } \mathbf{c}'\in\mathbb{R}^{\lambda} \tag{9}$$

so that:

$$\mathbf{v}_f = \mathbf{D}\dot{\boldsymbol{\zeta}} = \mathbf{D}\mathbf{J}^{\perp}\mathbf{c}' \tag{10}$$

By comparing Eqs. (8) and (10) and by choosing $\mathbf{c} = \mathbf{c}'$, we have:

$$\boldsymbol{\Xi}^{\perp} = \mathbf{D}\mathbf{J}^{\perp} \tag{11}$$

The coefficients $\mathbf{c}$ coincide with the free coordinates derivative $\dot{\boldsymbol{\zeta}}_f$, if $\boldsymbol{\Xi}^{\perp}$ (and thus $\mathbf{J}^{\perp}$, cf. Eq.(11)) is computed according to the following procedure. First, we partition the analytical Jacobian matrix $\mathbf{J}$ as:

$$\mathbf{J} = \boldsymbol{\Xi}\mathbf{D} = \boldsymbol{\Xi}\begin{bmatrix}\mathbf{D}_c & \mathbf{D}_f\end{bmatrix} = \begin{bmatrix}\boldsymbol{\Xi}\mathbf{D}_c & \boldsymbol{\Xi}\mathbf{D}_f\end{bmatrix} = \begin{bmatrix}\mathbf{J}_c & \mathbf{J}_f\end{bmatrix} \tag{12}$$

where $\mathbf{D}_c\in\mathbb{R}^{6\times n}$, $\mathbf{D}_f\in\mathbb{R}^{6\times\lambda}$, $\mathbf{J}_c = \boldsymbol{\Xi}\mathbf{D}_c\in\mathbb{R}^{n\times n}$, and $\mathbf{J}_f = \boldsymbol{\Xi}\mathbf{D}_f\in\mathbb{R}^{n\times\lambda}$. Matrix $\mathbf{J}^{\perp}$ can be symbolically computed under the assumption that $\mathrm{rank}(\mathbf{J}_c) = n$ and, thus, invertible. By assuming so[2], matrix $\mathbf{J}^{\perp}$ can be derived from Eq. (5) by setting $\dot{\mathbf{i}} = \mathbf{0}_{n\times 1}$:

$$\mathbf{J}\dot{\boldsymbol{\zeta}} = \mathbf{J}_c\dot{\boldsymbol{\zeta}}_c + \mathbf{J}_f\dot{\boldsymbol{\zeta}}_f = \mathbf{0}_{n\times 1} \qquad \Longrightarrow \qquad \dot{\boldsymbol{\zeta}}_c = -\mathbf{J}_c^{-1}\mathbf{J}_f\dot{\boldsymbol{\zeta}}_f \tag{13}$$

and finally:

$$\dot{\boldsymbol{\zeta}} = \begin{bmatrix}\dot{\boldsymbol{\zeta}}_c\\ \dot{\boldsymbol{\zeta}}_f\end{bmatrix} = \begin{bmatrix}-\mathbf{J}_c^{-1}\mathbf{J}_f\\ \mathbf{I}_{\lambda\times\lambda}\end{bmatrix}\dot{\boldsymbol{\zeta}}_f = \mathbf{J}^{\perp}\dot{\boldsymbol{\zeta}}_f, \qquad \mathbf{J}^{\perp} = \begin{bmatrix}-\mathbf{J}_c^{-1}\mathbf{J}_f\\ \mathbf{I}_{\lambda\times\lambda}\end{bmatrix} \tag{14}$$

$$\mathbf{v}_f = \mathbf{D}\dot{\boldsymbol{\zeta}} = \mathbf{D}\mathbf{J}^{\perp}\dot{\boldsymbol{\zeta}}_f = \boldsymbol{\Xi}^{\perp}\dot{\boldsymbol{\zeta}}_f, \qquad \boldsymbol{\Xi}^{\perp} = \mathbf{D}\mathbf{J}^{\perp} \tag{15}$$

[1] The free twist is derived in [18] and reported here in order to make the paper self contained.

[2] By suitably choosing controlled and free coordinates, it can be proven that this is always true for *UACDPR* [18], but the demonstration is omitted due to space limitation.

where $\mathbf{c} = \dot{\boldsymbol{\zeta}}_f$. It should be noted that the expression of $\dot{\boldsymbol{\zeta}}$ provided in Eq. (14) is valid *only when* $\dot{\mathbf{l}} = \mathbf{0}_{n\times 1}$.

The *controlled twist* is defined as the *EE* twist due to cable actuation only, that is, the twist resulting from a zero free-coordinate derivative, $\dot{\boldsymbol{\zeta}}_f = \mathbf{0}_{\lambda\times 1}$. The expression of $\mathbf{v}_c$ is determined by considering Eq. (4) and setting $\dot{\boldsymbol{\zeta}}_f = \mathbf{0}_{\lambda\times 1}$:

$$\mathbf{v}_c = \mathbf{D}\dot{\boldsymbol{\zeta}} = \begin{bmatrix}\mathbf{D}_c & \mathbf{D}_f\end{bmatrix}\begin{bmatrix}\dot{\boldsymbol{\zeta}}_c \\ \mathbf{0}_{\lambda\times 1}\end{bmatrix} = \begin{bmatrix}\mathbf{D}_c\dot{\boldsymbol{\zeta}}_c \\ \mathbf{0}_{\lambda\times 1}\end{bmatrix} \tag{16}$$

In addition, by recalling position (12):

$$\dot{\mathbf{l}} = \mathbf{J}\dot{\boldsymbol{\zeta}} = \begin{bmatrix}\mathbf{J}_c & \mathbf{J}_f\end{bmatrix}\begin{bmatrix}\dot{\boldsymbol{\zeta}}_c \\ \mathbf{0}_{\lambda\times 1}\end{bmatrix} \qquad \Longrightarrow \qquad \dot{\boldsymbol{\zeta}}_c = \mathbf{J}_c^{-1}\dot{\mathbf{l}} \tag{17}$$

and thus:

$$\mathbf{v}_c = \begin{bmatrix}\mathbf{D}_c\dot{\boldsymbol{\zeta}}_c \\ \mathbf{0}_{\lambda\times 1}\end{bmatrix} = \begin{bmatrix}\mathbf{D}_c\mathbf{J}_c^{-1}\dot{\mathbf{l}} \\ \mathbf{0}_{\lambda\times 1}\end{bmatrix} = \begin{bmatrix}\mathbf{D}_c\mathbf{J}_c^{-1} \\ \mathbf{0}_{\lambda\times n}\end{bmatrix}\dot{\mathbf{l}} = \boldsymbol{\Xi}^{\parallel}\dot{\mathbf{l}}, \qquad \boldsymbol{\Xi}^{\parallel} = \begin{bmatrix}\mathbf{D}_c\mathbf{J}_c^{-1} \\ \mathbf{0}_{\lambda\times n}\end{bmatrix} \in \mathbb{R}^{6\times n} \tag{18}$$

while an expression of $\dot{\boldsymbol{\zeta}}$ which is valid *only when* $\dot{\boldsymbol{\zeta}}_f = \mathbf{0}_{\lambda\times 1}$ is deduced from Eq. (17):

$$\dot{\boldsymbol{\zeta}} = \begin{bmatrix}\mathbf{J}_c^{-1} \\ \mathbf{0}_{\lambda\times n}\end{bmatrix}\dot{\mathbf{l}} = \mathbf{J}^{\parallel}\dot{\mathbf{l}}, \qquad \mathbf{J}^{\parallel} = \begin{bmatrix}\mathbf{J}_c^{-1} \\ \mathbf{0}_{\lambda\times n}\end{bmatrix}, \qquad \boldsymbol{\Xi}^{\parallel} = \mathbf{D}\mathbf{J}^{\parallel} \tag{19}$$

The newly defined matrix $\boldsymbol{\Xi}^{\parallel}$ has the property to be a right inverse for the kinematic Jacobian $\boldsymbol{\Xi}$, namely $\boldsymbol{\Xi}\boldsymbol{\Xi}^{\parallel} = \mathbf{I}_{n\times n}$, when $\dot{\boldsymbol{\zeta}}_f = \mathbf{0}_{\lambda\times 1}$. This can be verified by substituting Eq. (18) in (3):

$$\boldsymbol{\Xi}\mathbf{v}_c - \dot{\mathbf{l}} = \boldsymbol{\Xi}\boldsymbol{\Xi}^{\parallel}\dot{\mathbf{l}} - \dot{\mathbf{l}} = \mathbf{0}_{n\times 1} \qquad \Longrightarrow \qquad \boldsymbol{\Xi}\boldsymbol{\Xi}^{\parallel} = \mathbf{I}_{n\times n} \tag{20}$$

Finally, one has:

$$\mathbf{v} = \mathbf{v}_f + \mathbf{v}_c = \boldsymbol{\Xi}^{\perp}\dot{\boldsymbol{\zeta}}_f + \boldsymbol{\Xi}^{\parallel}\dot{\mathbf{l}} \tag{21}$$

It can be verified that the expression of $\mathbf{v}$ in Eq. (21) verifies the *EE* first-order kinematics expressed in Eq. (3):

$$\boldsymbol{\Xi}\mathbf{v} - \dot{\mathbf{l}} = \boldsymbol{\Xi}\left(\boldsymbol{\Xi}^{\perp}\dot{\boldsymbol{\zeta}}_f + \boldsymbol{\Xi}^{\parallel}\dot{\mathbf{l}}\right) - \dot{\mathbf{l}} = \underbrace{\boldsymbol{\Xi}\boldsymbol{\Xi}^{\perp}}_{\mathbf{0}_{n\times\lambda}}\dot{\boldsymbol{\zeta}}_f + \underbrace{\boldsymbol{\Xi}\boldsymbol{\Xi}^{\parallel}}_{\mathbf{I}_{n\times n}}\dot{\mathbf{l}} - \dot{\mathbf{l}} = \mathbf{0}_{n\times 1} \tag{22}$$

At last, the complete expression of the pose derivative can be written as:

$$\dot{\boldsymbol{\zeta}} = \mathbf{J}^{\perp}\dot{\boldsymbol{\zeta}}_f + \mathbf{J}^{\parallel}\dot{\mathbf{l}} \tag{23}$$

2.3 Static Modelling

The static model of the *EE* is determined by considering that cable tensions counteract the external actions applied onto the *EE*. If we consider gravity as the only load applied to the *EE* center of mass *G*, the static equilibrium yields (see Fig. 1):

$$\boldsymbol{\Xi}^T\boldsymbol{\tau} = \mathbf{f}, \qquad \mathbf{f} = \begin{bmatrix}\boldsymbol{\phi} \\ \mathbf{0}_{3\times 1}\end{bmatrix} \tag{24}$$

where $\boldsymbol{\phi} = m\mathbf{g}$, m is the *EE* mass, $\mathbf{g}$ is the gravitational acceleration, and $\boldsymbol{\tau} = [\tau_1, \cdots, \tau_n]^T$ is the array containing the cable tensions.

The static constraint that the *EE* coordinates must statify at equilibrium (regardless of the sign of cable tensions), is obtained by pre-multiplying Eq. (24) by ${\Xi^{\perp}}^T$:

$$ {\Xi^{\perp}}^T \Xi^T \boldsymbol{\tau} = \mathbf{0}_{\lambda \times 1} = {\Xi^{\perp}}^T \mathbf{f} \tag{25} $$

where ${\Xi^{\perp}}^T \Xi^T = \mathbf{0}_{\lambda \times n}$ by definition of nullspace. Cable tensions can be computed by pre-multiplying Eq. (24) by ${\Xi^{\parallel}}^T$, instead:

$$ {\Xi^{\parallel}}^T \Xi^T \boldsymbol{\tau} = \boldsymbol{\tau} = {\Xi^{\parallel}}^T \mathbf{f} \tag{26} $$

The geometrico-static model is established by considering Eq. (1) for $i = 1, \ldots, n$ and Eq. (25):

$$ \begin{cases} \boldsymbol{\rho} \cdot \boldsymbol{\rho} - l_1^2 = 0 \\ \vdots \\ \boldsymbol{\rho} \cdot \boldsymbol{\rho} - l_n^2 = 0 \\ {\Xi^{\perp}}^T \mathbf{f} = \mathbf{0}_{\lambda \times 1} \end{cases} \tag{27} $$

The non-linear system (27) has 6 equations in $6 + n$ unknowns, namely the 6 *EE* coordinates $\boldsymbol{\zeta}$ and the n cable lengths $\mathbf{l}$. By assigning $\mathbf{l}$, the forward geometrico-static problem is established; if instead $\boldsymbol{\zeta}_c$ is assigned, the inverse geometrico-static problem is determined. Both problems are well-posed, since the system (27) has 6 equations in 6 unknowns, and they may admit multiple real solutions: a solution is acceptable if cable tensions, obtained from Eq. (26), are strictly positive, and the equilibrium is stable [1].

3 Maximum Tension Variation under a Cable Displacement Error

In this section, the *maximum tension variation under a cable displacement error*, denoted by $\sigma_{\tau\%,\infty}$, is formulated by considering how cable length variations, or errors, influence cable tensions around equilibrium.

The equilibrium of a *UACDPR* may vary for two reasons, namely a change of cable lengths or external wrench. In this paper, we only consider the former. By differentiating Eq. (26), we evaluate how tensions vary due to pose variations:

$$ \mathrm{d}\boldsymbol{\tau} = \mathrm{d}\left({\Xi^{\parallel}}^T \mathbf{f}\right) = \frac{\partial\left({\Xi^{\parallel}}^T \mathbf{f}\right)}{\partial \boldsymbol{\zeta}} \mathrm{d}\boldsymbol{\zeta} \tag{28} $$

If we consider $\Xi^T \boldsymbol{\tau} = \mathbf{f}$, the partial derivative in Eq. (28) is:

$$ \frac{\partial\left({\Xi^{\parallel}}^T \mathbf{f}\right)}{\partial \boldsymbol{\zeta}} = \left(\frac{\partial {\Xi^{\parallel}}^T}{\partial \boldsymbol{\zeta}} \mathbf{f} + {\Xi^{\parallel}}^T \frac{\partial \mathbf{f}}{\partial \boldsymbol{\zeta}}\right) = \left(\frac{\partial {\Xi^{\parallel}}^T}{\partial \boldsymbol{\zeta}} \Xi^T \boldsymbol{\tau} + {\Xi^{\parallel}}^T \frac{\partial \mathbf{f}}{\partial \boldsymbol{\zeta}}\right) \tag{29} $$

$$\frac{\partial\left(\Xi^{\parallel^T}\mathbf{f}\right)}{\partial\boldsymbol{\zeta}} = -\left(\Xi^{\parallel^T}\frac{\partial\Xi^T}{\partial\boldsymbol{\zeta}}\boldsymbol{\tau} - \Xi^{\parallel^T}\frac{\partial\mathbf{f}}{\partial\boldsymbol{\zeta}}\right) = -\Xi^{\parallel^T}\left[\sum_{i=1}^{n}\left(\tau_i\frac{\partial\boldsymbol{\xi}_i}{\partial\boldsymbol{\zeta}}\right) - \frac{\partial\mathbf{f}}{\partial\boldsymbol{\zeta}}\right] \tag{30}$$

where we have taken into consideration that, since $\Xi^{\parallel^T}\Xi^T = \mathbf{I}_{n\times n}$:

$$\frac{\partial\Xi^{\parallel^T}}{\partial\boldsymbol{\zeta}}\Xi^T + \Xi^{\parallel^T}\frac{\partial\Xi^T}{\partial\boldsymbol{\zeta}} = \mathbf{0}_{n\times n} \tag{31}$$

It can be shown by computation that Eq. (30) can be rewritten as[3]:

$$\frac{\partial\left(\Xi^{\parallel^T}\mathbf{f}\right)}{\partial\boldsymbol{\zeta}} = -\Xi^{\parallel^T}\mathbf{K}\mathbf{D} \tag{32}$$

$$\mathbf{K} = \sum_{i=1}^{n}\frac{\tau_i}{l_i}\begin{bmatrix}\mathbf{T}_i & -\mathbf{T}_i\tilde{\mathbf{a}}_i' \\ \tilde{\mathbf{a}}_i'\mathbf{T}_i & -\tilde{\mathbf{a}}_i'\mathbf{T}_i\tilde{\mathbf{a}}_i'\end{bmatrix}, \qquad \mathbf{T}_i = \mathbf{I}_{3\times3} - \mathbf{t}_i\mathbf{t}_i^T \tag{33}$$

where $\tilde{(\cdot)}$ denotes the skew-symmetric representation of a vector. Matrix $\mathbf{K}$ is referred to as *Geometric Stiffness* of the *CDPR* [18, 19], because it depends on geometry, and it is fundamentally different from the so-called *Passive Stiffness* generated by cable deformations (not considered in this paper).

From Eq. (23), we infer that the pose variation $\mathrm{d}\boldsymbol{\zeta}$ in Eq. (28) is produced by a variation of either cable lengths or free-pose coordinates, namely:

$$\mathrm{d}\boldsymbol{\zeta} = \mathbf{J}^{\perp}\mathrm{d}\boldsymbol{\zeta}_f + \mathbf{J}^{\parallel}\mathrm{d}\mathbf{l} \tag{34}$$

On the other hand, the variation of free coordinates is not independent, since Eq. (25) must hold in the newly attained equilibrium. Thus, the free-coordinate variation upon a cable-length change can be determined by differentiating Eq. (25):

$$\mathrm{d}\left(\Xi^{\perp^T}\mathbf{f}\right) = \frac{\partial\left(\Xi^{\perp^T}\mathbf{f}\right)}{\partial\boldsymbol{\zeta}}\mathrm{d}\boldsymbol{\zeta} = \mathbf{0}_{\lambda\times1} \tag{35}$$

If we substitute Eq. (34) in Eq. (35), we obtain:

$$\mathrm{d}\left(\Xi^{\perp^T}\mathbf{f}\right) = \frac{\partial\left(\Xi^{\perp^T}\mathbf{f}\right)}{\partial\boldsymbol{\zeta}}\mathbf{J}^{\perp}\mathrm{d}\boldsymbol{\zeta}_f + \frac{\partial\left(\Xi^{\perp^T}\mathbf{f}\right)}{\partial\boldsymbol{\zeta}}\mathbf{J}^{\parallel}\mathrm{d}\mathbf{l} = \mathbf{0}_{\lambda\times1} \tag{36}$$

Since $\Xi^T\boldsymbol{\tau} = \mathbf{f}$ at equilibrium, the partial derivative in Eq. (36) is:

$$\frac{\partial\left(\Xi^{\perp^T}\mathbf{f}\right)}{\partial\boldsymbol{\zeta}} = \left(\frac{\partial\Xi^{\perp^T}}{\partial\boldsymbol{\zeta}}\mathbf{f} + \Xi^{\perp^T}\frac{\partial\mathbf{f}}{\partial\boldsymbol{\zeta}}\right) = \left(\frac{\partial\Xi^{\perp^T}}{\partial\boldsymbol{\zeta}}\Xi^T\boldsymbol{\tau} + \Xi^{\perp^T}\frac{\partial\mathbf{f}}{\partial\boldsymbol{\zeta}}\right) \tag{37}$$

$$\frac{\partial\left(\Xi^{\perp^T}\mathbf{f}\right)}{\partial\boldsymbol{\zeta}} = -\left(\Xi^{\perp^T}\frac{\partial\Xi^T}{\partial\boldsymbol{\zeta}}\boldsymbol{\tau} - \Xi^{\perp^T}\frac{\partial\mathbf{f}}{\partial\boldsymbol{\zeta}}\right) = -\Xi^{\perp^T}\left(\frac{\partial\Xi^T}{\partial\boldsymbol{\zeta}}\boldsymbol{\tau} - \frac{\partial\mathbf{f}}{\partial\boldsymbol{\zeta}}\right) \tag{38}$$

[3] Detailed computation of $\mathbf{K}$ is reported in [18] for a more general case, i.e. when cables are guided by swivel pulleys and an arbitrary external wrench is applied to the *EE*.

where we have taken into consideration that, since $\boldsymbol{\Xi}^{\perp^T}\boldsymbol{\Xi}^T = \mathbf{0}_{\lambda\times n}$:

$$\frac{\partial\boldsymbol{\Xi}^{\perp^T}}{\partial\boldsymbol{\zeta}}\boldsymbol{\Xi}^T + \boldsymbol{\Xi}^{\perp^T}\frac{\partial\boldsymbol{\Xi}^T}{\partial\boldsymbol{\zeta}} = \mathbf{0}_{\lambda\times n} \tag{39}$$

and ultimately (cf. Eqs. (30) and (32)):

$$\frac{\partial\left(\boldsymbol{\Xi}^{\perp^T}\mathbf{f}\right)}{\partial\boldsymbol{\zeta}} = -\boldsymbol{\Xi}^{\perp^T}\mathbf{K}\mathbf{D} \tag{40}$$

By substituting Eq. (40) in Eq. (36), and considering Eqs. (19) and (15), one obtains:

$$\boldsymbol{\Xi}^{\perp^T}\mathbf{K}\mathbf{D}\mathbf{J}^{\perp}\mathrm{d}\boldsymbol{\zeta}_f + \boldsymbol{\Xi}^{\perp^T}\mathbf{K}\mathbf{D}\mathbf{J}^{\parallel}\mathrm{d}\mathbf{l} = \mathbf{K}_f^{\perp}\mathrm{d}\boldsymbol{\zeta}_f + \mathbf{K}_l^{\perp}\mathrm{d}\mathbf{l} = \mathbf{0}_{\lambda\times 1} \tag{41}$$

where:

$$\mathbf{K}_f^{\perp} = \boldsymbol{\Xi}^{\perp^T}\mathbf{K}\boldsymbol{\Xi}^{\perp} \in \mathbb{R}^{\lambda\times\lambda}, \qquad \mathbf{K}_l^{\perp} = \boldsymbol{\Xi}^{\perp^T}\mathbf{K}\boldsymbol{\Xi}^{\parallel} \in \mathbb{R}^{\lambda\times n} \tag{42}$$

Note that, if the equilibrium is stable, $\mathbf{K}_f^{\perp}$ is positive definite, thus invertible [18].

Then, the free-coordinate variation upon a variation of cable lengths is:

$$\mathrm{d}\boldsymbol{\zeta}_f = -\mathbf{K}_f^{-\perp}\mathbf{K}_l^{\perp}\mathrm{d}\mathbf{l} \tag{43}$$

and substituting Eq. (43) in Eq. (34) the overall pose variation is determined as:

$$\mathrm{d}\boldsymbol{\zeta} = \left(-\mathbf{J}^{\perp}\mathbf{K}_f^{-\perp}\mathbf{K}_l^{\perp} + \mathbf{J}^{\parallel}\right)\mathrm{d}\mathbf{l} \tag{44}$$

In the end, the variation of cable tension upon a change of the cable lengths is evaluated by substituting Eq. (32) and (44) into Eq. (28):

$$\mathrm{d}\boldsymbol{\tau} = -\boldsymbol{\Xi}^{\parallel^T}\mathbf{K}\mathbf{D}\left(-\mathbf{J}^{\perp}\mathbf{K}_f^{-\perp}\mathbf{K}_l^{\perp} + \mathbf{J}^{\parallel}\right)\mathrm{d}\mathbf{l} = \mathbf{K}_{\tau}\mathrm{d}\mathbf{l} \tag{45}$$

$$\mathbf{K}_{\tau} = -\boldsymbol{\Xi}^{\parallel^T}\mathbf{K}\left(-\boldsymbol{\Xi}^{\perp}\mathbf{K}_f^{-\perp}\mathbf{K}_l^{\perp} + \boldsymbol{\Xi}^{\parallel}\right) \tag{46}$$

Finally, the *maximum tension variation under a cable displacement error* $\sigma_{\tau\%,\infty}$ is defined as:

$$\sigma_{\tau\%,\infty} = \max_{\|\mathbf{dl}\|_{\infty}=1} \|\mathrm{d}\boldsymbol{\tau}_{\%}\|_{\infty} \tag{47}$$

where $\mathrm{d}\boldsymbol{\tau}_{\%} = 100[(\mathrm{d}\tau_1)/\tau_1, \cdots, (\mathrm{d}\tau_n)/\tau_n]$ is the percentage tension error, and $\|\cdot\|_{\infty}$ indicates the vector ∞-norm. As highlighted in [20], the use of the infinity-norm attains the clearest physical meaning, since it is consistent with a realistic actuation error model, namely $-\mathrm{d}l_{i,\max} \le \mathrm{d}l_i \le \mathrm{d}l_{i,\max}$ for $i = 1,\ldots,n$. The definition of the index based on the percentage variation of cable tensions, and not on their absolute variation, is justified by the fact that a small tension variation on an almost slack cable is comparably relevant to a large tension variation on a well-taut cable.

By considering Eq. (45) and the definitions of matrix norms [21], we have:

$$\sigma_{\tau\%,\infty} = \max_{\|\mathbf{dl}\|_{\infty}=1} \|\mathrm{d}\boldsymbol{\tau}_{\%}\|_{\infty} = \|\mathbf{K}_{\tau\%}\|_{\infty} \tag{48}$$

where $\mathbf{K}_{\tau\%}$ is, by accounting for Eq. (46):

$$\mathbf{K}_{\tau\%} = 100\mathbf{T}\mathbf{K}_{\tau}, \qquad \mathbf{T} = \mathrm{diag}(\boldsymbol{\tau})^{-1} \tag{49}$$

Note that the computation of the infinity norm of a matrix is straightforward, as it consists of computing the 1-norms of its row vectors and choosing the largest.

Notice that $\sigma_{\tau\%,\infty}$ is not dimensionless. If cable lengths are expressed in millimeters, $\sigma_{\tau\%,\infty}$ is the percentage error on the estimated cable tension if a control error of at the most 1mm occurs in cable lengths.

4 Application

As an application of the proposed performance index, we optimize the static orientation of a 4-cable *UACDPR EE* that has to perform a positioning task. Since only 3 of the 4 controllable coordinates of the robot needs to be assigned to perform the task, it is reasonable to investigate which orientation among the possibly infinite ones attainable by *EE* would locally optimize the performance of the robot. Then, for an assigned *EE* position, its orientation may be determined as the one minimizing $\sigma_{\tau\%,\infty}$, so that, should cable lengths not be perfectly controlled by the robot, the risk of cables becoming slack is minimized.

Consider a *UACDPR* with the following parameters:

$$^{P}\mathbf{a}_1 = \begin{bmatrix} 0.2 \\ 0.3 \\ 0.3 \end{bmatrix} \mathrm{m}, \quad ^{P}\mathbf{a}_2 = \begin{bmatrix} 0.2 \\ -0.3 \\ 0.3 \end{bmatrix} \mathrm{m}, \quad ^{P}\mathbf{a}_3 = \begin{bmatrix} -0.2 \\ -0.3 \\ 0.3 \end{bmatrix} \mathrm{m}, \quad ^{P}\mathbf{a}_4 = \begin{bmatrix} -0.2 \\ 0.3 \\ 0.3 \end{bmatrix} \mathrm{m},$$

$$\mathbf{b}_1 = \begin{bmatrix} 1.5 \\ 1 \\ 0 \end{bmatrix} \mathrm{m}, \quad \mathbf{b}_2 = \begin{bmatrix} 1.5 \\ -1 \\ 0 \end{bmatrix} \mathrm{m}, \quad \mathbf{b}_3 = \begin{bmatrix} -1.5 \\ -1 \\ 0 \end{bmatrix} \mathrm{m}, \quad \mathbf{b}_4 = \begin{bmatrix} -1.5 \\ 1 \\ 0 \end{bmatrix} \mathrm{m}, \quad m = 1\mathrm{Kg}$$

and the position $\mathbf{p}_0 = [0\,0\,-2]^T\,\mathrm{m}$ that the *EE* has to reach. Orientation $\boldsymbol{\epsilon}$ is parametrized with *Roll-Pitch-Yaw* Euler angles, namely the *EE* rotation matrix is $\mathbf{R}(\boldsymbol{\epsilon}) = \mathbf{R}_z(\phi)\mathbf{R}_y(\theta)\mathbf{R}_x(\chi)$, with $\mathbf{R}_i$, $i = x, y, z$ being elementary rotation matrices.

The optimal orientation of the *EE* is determined by solving the non-linear constrained optimization:

$$\boldsymbol{\epsilon}_{opt} = \min_{\boldsymbol{\epsilon}} \sigma_{\tau\%,\infty}(\boldsymbol{\epsilon}) \tag{50}$$

subject to:

$$\boldsymbol{\Xi}^{\perp^T}\mathbf{f} = \mathbf{0}_{\lambda\times 1} \qquad \text{and} \qquad \boldsymbol{\tau} \succeq \tau_{min} \tag{51}$$

where $\succeq$ denotes element-wise inequality, and $\tau_{min} = 2\mathrm{N}$ is the inferior tension limit. The model presented in this paper was implemented in Matlab, and Eq. (50) was solved by the *fmincon* function. The results are reported in Table 1.

Equilibrium orientations in the neighbourhood of the optimal one were also investigated, in order to understand the entity of the variation of $\sigma_{\tau\%,\infty}$ in the assigned $\mathbf{p}_0$. Accordingly, angle ϕ was continuously varied around ϕ_{opt}, while θ and χ were determined as the solutions of the inverse geometrico-static problem in Eq. (27). The

$\boldsymbol{\epsilon}$ [rad]	$\mathbf{l}$ [m]	$\boldsymbol{\tau}$ [N]	$\sigma_{\tau\%,\infty}$ [%/m]
$[0,0,0]^T$	$[2.252,2.252,2.252,2.252]^T$	$[3.25,3.25,3.25,3.25]^T$	2117

Table 1: Optimization results in $\mathbf{p}_0$

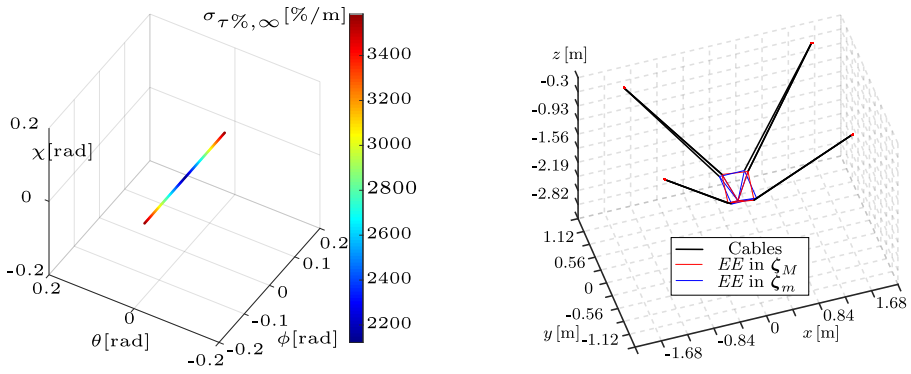

(a) $\sigma_{\tau\%,\infty}$ [%/m] *for* $\mathbf{p}_0$

(b) EE *configurations in* $\mathbf{p}_0$

Fig. 2: *Simulation results for* $\mathbf{p}_0$

results of this analysis are reported in Fig. 2a, and, in the authors' opinion, one detail is particularly interesting. The worst (highest) values of $\sigma_{\tau\%,\infty}$ are obtained for those equilibrium orientations that results in one cable reaching the lower tension limit τ_{min}: even though $\sigma_{\tau\%,\infty}$ does not vary considerably in the assigned position of the *EE*, the highest value of this index, where one cable is the least tense, implies that those configurations are intrinsically not safe to reach if cable lengths are not perfectly controlled, since one cable may become slack.

In order to emphasize why this result is critical, consider two equilibrium orientations $\boldsymbol{\epsilon}_M$ and $\boldsymbol{\epsilon}_m$ attainable by the *UACDPR* in $\mathbf{p}_0$, respectively maximizing and minimizing $\sigma_{\tau\%,\infty}$ (see Fig. 2b, and note that the subscript M and m will be used to denote all variables associated with such orientations):

$$\boldsymbol{\zeta}_M = \begin{bmatrix} 0 \\ 0 \\ -2 \\ -0.161 \\ 0 \\ 0 \end{bmatrix} [\text{m,rad}], \quad \mathbf{l}_M = \begin{bmatrix} 2.237 \\ 2.273 \\ 2.237 \\ 2.273 \end{bmatrix} \text{m}, \quad \boldsymbol{\tau}_M = \begin{bmatrix} 4.48 \\ 2 \\ 4.48 \\ 2 \end{bmatrix} \text{N}, \quad \sigma_{\tau\%,\infty,M} = 3615\,\%/\text{m}$$

$$\boldsymbol{\zeta}_m = \begin{bmatrix} 0 \\ 0 \\ -2 \\ 0 \\ 0 \\ 0 \end{bmatrix} [\text{m,rad}], \quad \mathbf{l}_m = \begin{bmatrix} 2.252 \\ 2.252 \\ 2.252 \\ 2.252 \end{bmatrix} \text{m}, \quad \boldsymbol{\tau}_m = \begin{bmatrix} 3.25 \\ 3.25 \\ 3.25 \\ 3.25 \end{bmatrix} \text{N}, \quad \sigma_{\tau\%,\infty,m} = 2117\,\%/\text{m}$$

Suppose now that the second and the fourth cable are 1cm longer than their values in $\mathbf{l}_M$ and $\mathbf{l}_m$: these new cable lengths are denoted as $\mathbf{l}_M^\star$ and $\mathbf{l}_m^\star$, respectively. The solutions to the forward geometrico-static problem for $\mathbf{l}_M^\star$ and $\mathbf{l}_m^\star$ are:

$$\boldsymbol{\zeta}_M^\star = \begin{bmatrix} 0 \\ 0 \\ -2.004 \\ -0.207 \\ 0 \\ 0 \end{bmatrix} [\text{m}, \text{rad}], \quad \mathbf{l}_M^\star = \begin{bmatrix} 2.237 \\ 2.283 \\ 2.237 \\ 2.283 \end{bmatrix} \text{m}, \quad \boldsymbol{\tau}_M^\star = \begin{bmatrix} 4.85 \\ 1.63 \\ 4.85 \\ 1.63 \end{bmatrix} \text{N}$$

$$\boldsymbol{\zeta}_m^\star = \begin{bmatrix} 0 \\ 0 \\ -2.006 \\ -0.045 \\ 0 \\ 0 \end{bmatrix} [\text{m}, \text{rad}], \quad \mathbf{l}_m^\star = \begin{bmatrix} 2.252 \\ 2.262 \\ 2.252 \\ 2.262 \end{bmatrix} \text{m}, \quad \boldsymbol{\tau}_m^\star = \begin{bmatrix} 3.59 \\ 2.90 \\ 3.59 \\ 2.90 \end{bmatrix} \text{N}$$

It is clear that for the pose associated with $\mathbf{l}_M^\star$ cable tensions drop below the tension limit, while for the pose associated with $\mathbf{l}_m^\star$ this issues does not occur.

5 Conclusions

In this paper, a novel index $\sigma_{\tau\%,\infty}$ for the evaluation of geometrico-static performances of *UACDPRs*, called *maximum tension variation under a cable displacement error*, was introduced and analitically derived. Its relevance was demonstrated on a 4-cable *UACDPR*, by determining the orientations minimizing and maximizing said index when the position of the *EE* is assigned. It was shown that, in case cable lengths corresponding to minimal and maximal values of $\sigma_{\tau\%,\infty}$ exhibit errors, the risk of loosing tension in one cable is the highest in the latter configuration.

In the future, this index will be used for the characterizing and optimizing *UACDPRs* reachable workspace.

References

1. M. Carricato and J. Merlet, "Stability Analysis of Underconstrained Cable-Driven Parallel Robots," *IEEE Transactions on Robotics*, vol. 29, no. 1, pp. 288–296, Feb 2013.
2. J. Fink, N. Michael, S. Kim, and V. Kumar, "Planning and control for cooperative manipulation and transportation with aerial robots," *The International Journal of Robotics Research*, vol. 30, no. 3, pp. 324–334, 2011.
3. N. Zoso and C. Gosselin, "Point-to-point motion planning of a parallel 3-dof underactuated cable-suspended robot," in *2012 IEEE International Conference on Robotics and Automation*, May 2012, pp. 2325–2330.
4. E. Idà, T. Bruckmann, and M. Carricato, "Rest-to-rest trajectory planning for underactuated cable-driven parallel robots," *IEEE Transactions on Robotics*, vol. 35, no. 6, pp. 1338–1351, Dec 2019.

5. E. Idà, S. Briot, and M. Carricato, "Robust trajectory planning of under-actuated cable-driven parallel robot with 3 cables," in *Advances in Robot Kinematics 2020*, J. Lenarčič and B. Siciliano, Eds. Cham: Springer International Publishing, 2021, pp. 65–72.
6. G. Abbasnejad and M. Carricato, "Direct geometrico-static problem of underconstrained cable-driven parallel robots with n cables," *IEEE Transactions on Robotics*, vol. 31, no. 2, pp. 468–478, April 2015.
7. M. Zarei, A. Aflakian, A. Kalhor, and M. T. Masouleh, "Oscillation damping of nonlinear control systems based on the phase trajectory length concept: An experimental case study on a cable-driven parallel robot," *Mechanism and Machine Theory*, vol. 126, pp. 377 – 396, 2018.
8. E. Idá, J.-P. Merlet, and M. Carricato, "Automatic self-calibration of suspended under-actuated cable-driven parallel robot using incremental measurements," in *Cable-Driven Parallel Robots*, A. Pott and T. Bruckmann, Eds. Cham: Springer International Publishing, 2019, pp. 333–344.
9. A. A. Kumar, J.-F. Antoine, P. Zattarin, and G. Abba, "Workspace analysis of a 4 cable-driven spatial parallel robot," in *ROMANSY 22 – Robot Design, Dynamics and Control*, V. Arakelian and P. Wenger, Eds. Cham: Springer International Publishing, 2019, pp. 204–212.
10. S. Patel and T. Sobh, "Manipulator performance measures - a comprehensive literature survey," *Journal of Intelligent & Robotic Systems*, vol. 77, no. 3, pp. 547–570, 2015.
11. J. Pusey, A. Fattah, S. Agrawal, and E. Messina, "Design and workspace analysis of a 6-6 cable-suspended parallel robot," *Mechanism and Machine Theory*, vol. 39, no. 7, pp. 761 – 778, 2004.
12. G. Mottola, C. Gosselin, and M. Carricato, "Effect of actuation errors on a purely-translational spatial cable-driven parallel robot," in *2019 IEEE 9th Annual International Conference on CYBER Technology in Automation, Control, and Intelligent Systems (CYBER)*, 2019, pp. 701–707.
13. E. Idà, D. Marian, and M. Carricato, "A deployable cable-driven parallel robot with large rotational capabilities for laser-scanning applications," *IEEE Robotics and Automation Letters*, vol. 5, no. 3, pp. 4140–4147, July 2020.
14. R. Verhoeven and M. Hiller, "Tension distribution in tendon-based stewart platforms," in *Advances in Robot Kinematics*. Springer, 2002, pp. 117–124.
15. C. B. Pham, S. H. Yeo, G. Yang, and I.-M. Chen, "Workspace analysis of fully restrained cable-driven manipulators," *Robotics and Autonomous Systems*, vol. 57, no. 9, pp. 901–912, 2009.
16. M. Gouttefarde, J. Collard, N. Riehl, and C. Baradat, "Geometry selection of a redundantly actuated cable-suspended parallel robot," *IEEE Transactions on Robotics*, vol. 31, no. 2, pp. 501–510, 2015.
17. G. Boschetti and A. Trevisani, "Cable robot performance evaluation by wrench exertion capability," *Robotics*, vol. 7, no. 2, 2018.
18. E. Idà, S. Briot, and M. Carricato, "Natural oscillations of underactuated cable-driven parallel robots," *IEEE Access*, pp. 1–1, 2021.
19. D. Surdilovic, J. Radojicic, and J. Krüger, "Geometric stiffness analysis of wire robots: A mechanical approach," in *Cable-Driven Parallel Robots*, T. Bruckmann and A. Pott, Eds. Berlin, Heidelberg: Springer Berlin Heidelberg, 2013, pp. 389–404.
20. J. P. Merlet, "Jacobian, Manipulability, Condition Number, and Accuracy of Parallel Robots," *Journal of Mechanical Design*, vol. 128, no. 1, pp. 199–206, 06 2005.
21. G. H. Golub and C. F. Van Loan, "Matrix computations, 4th," *Johns Hopkins*, 2013.